JOURNAL OF GEOPHYSICAL RESEARCH, VOL. 105, NO. D21, PAGES 26,555–26,567, NOVEMBER 16, 2000

Ultrafine particle size distributions measured in aircraft exhaust plumes

Charles A. Brock[1]

Department of Engineering, University of Denver, Denver, Colorado

Franz Schröder, Bernd Kärcher, Andreas Petzold,
Reinhold Busen, and Markus Fiebig

Institut für Physik der Atmosphäre, Deutsche Luft- und Raumfahrt, Oberpfaffenhofen, Wessling, Germany

Abstract. Fast-response measurements of particle size distributions were made for the first time in the near-field plume of a Boeing 737-300 aircraft burning fuel with fuel sulfur (S) contents (FSCs) of 56 and 2.6 ppmm, as well as in fresh and dissipating contrails from the same aircraft, using nine particle counters operating in parallel. Nonsoot particles were present in high concentrations, with number maxima at diameters ≤3 nm. From these and ancillary measurements we determined the apparent emission index, EI^*, or amount produced per kilogram of fuel burned, for particle number, surface, and volume, and the value of η^*, the apparent fraction of fuel S found in the particulate phase in the plume assuming the particles were composed of sulfuric acid and water. All of these parameters were functions of the age of the plume since emission, FSC, and presence or absence of contrail. The measurements support the use of values of η^* of <10% in numerical models of the effects of the current aircraft fleet on the atmosphere, suggest that non-S species become important contributors to particulate mass at very low FSCs, and place significant constraints on numerical models of plume microphysical processes.

1. Introduction

Current subsonic aircraft, as well as a proposed supersonic fleet, have the potential to significantly perturb atmospheric chemistry and climate. Aircraft directly emit soot particles with sizes >10 nm, and small (<10 nm diameter) particles volatile at temperatures >190°C are additionally formed in the near-field plume by condensation of gas-phase species [*Penner et al.*, 1999; *Kawa*, 1999]. The aerosol particles that are produced by aircraft may play a role as ice-forming nuclei for cirrus formation [*Jensen and Toon*, 1997] and are involved in the formation of contrails [*Schumann et al.*, 1996; *Gierens and Schumann*, 1996; *Petzold et al.*, 1997; *Schröder et al.*, 1998; *Kärcher et al.*, 1998b]. The relatively tenuous stratospheric aerosol may be significantly affected by aircraft emissions, particularly if a large supersonic fleet operates in the future at altitudes above 18 km, as has been proposed [*Kawa*, 1999].

Fahey et al. [1995] reported emission indices (EIs, quantity produced per kilogram of fuel consumed) for particle number in the wake of a Concorde aircraft in supersonic flight in the stratosphere. Fahey et al. concluded that, if a large supersonic fleet were to produce particles as did the Concorde, the particle surface area available for heterogeneous chemistry in the stratosphere would be significantly increased. In the Fahey et al. study the particles were presumed to be composed of sulfuric acid and water, and their size was not directly measured, but was estimated from the response characteristics of the condensation nucleus counter (CNC) used to detect and count the particles. Within these assumptions and measurement constraints, and with a measurement of the fuel S content of the Concorde's fuel in hand, they estimated that, at a minimum, 12% of the sulfur in the fuel must have been converted to particulate mass within 1 hour of emission. Further analyses of data from the Concorde intercept [*Kärcher and Fahey*, 1997; *Yu and Turco*, 1997] found that at least 20% of the fuel S must have been converted to condensable H_2SO_4 in the plume to explain the observations.

Measurements of OH in the Concorde plume were shown to place limits on the amount of in-plume oxidation of gaseous SO_2 that could be converted via the rate-limiting step in the formation of H_2SO_4, $SO_2+OH \xrightarrow{M} HSO_3$ [*Hanisco et al.*, 1997]. For the specific Concorde case studied by Fahey *et al.* [1995], only 2% or less of the fuel S emitted as SO_2 could have been oxidized via this pathway. This implies that significant fractions (>10%) of fuel S had to have been emitted as S(VI) compounds which rapidly reacted and condensed to form particles in the plume. Such high S(VI) EIs are at odds with simulations of chemistry in aircraft engines, which generally suggest a few to several percent of fuel S can be oxidized to form S(VI) compounds prior to emission [*Brown et al.*, 1996b; *Lukachko et al.*, 1998; *Tremmel and Schumann*, 1999]. Numerical studies of the possible consequences of a large, supersonic fleet on

[1]Also at Aeronomy Laboratory, National Oceanic and Atmospheric Administration, Boulder, Colorado, and the Cooperative Institute for Research in the Environmental Sciences, University of Colorado, Boulder, Colorado.

Copyright 2000 by the American Geophysical Union.

Paper number 2000JD900360.
0148-0227/00/2000JD900360$09.00

stratospheric chemistry find a large sensitivity to the fraction of S in fuel that is converted to small particles in the aircraft plume prior to dispersion to the global scale [*Weisenstein et al.*, 1998; *Kawa*, 1999]. Thus determining the mechanisms of S oxidation in aircraft engines is necessary to predict the environmental consequences of a future, supersonic fleet of aircraft.

The atmospheric implications of aircraft particle emissions reported by *Fahey et al.* [1995] have led to several studies regarding the emission and formation of particles and S compounds from modern commercial and military aircraft engines. Of these, the Sulfur-5 experiment [*Schröder et al.*, 1998; *Kärcher et al.*, 1998a; *Yu et al.*, 1998], the Subsonic Assessment: Cloud and Contrail Effects Special Study (SUCCESS), and the Subsonic Assessment: Near-Field Interactions Flights (SNIF) [*Miake-Lye et al.*, 1998; *Anderson et al.*, 1998a, 1998b], made particular progress in understanding small particle emissions and formation in plumes. These studies included improved size resolution of the ultrafine particles found in aircraft plumes.

Although the several studies of aircraft emissions associated with particle production encompass a wide range of engine types, fuel sources, and operating conditions, the findings can be summarized as follows:

1. Studies in aircraft engine test cells indicate that <10% of the emissions at the engine exit plane are in the form of SO_3 [*Wey et al.*, 1998]; direct measurements of S(VI) compounds in flight are few but indicate similar results [*Curtius et al.*, 1998; *Miake-Lye et al.*, 1998].

2. Small, volatile particles are not produced in significant concentrations during ground-based tests, but appear to be formed only in the plumes of flying aircraft [Anderson *et al.*, 1998a; *Paladino et al.*, 1998; *Petzold et al.*, 1997].

3. As the fuel sulfur content (FSC) increases, the apparent emission index, EI^*, of volatile particles produced in aircraft plumes and detected by CNC instruments with specified minimum detectable diameters increases [*Schumann et al.*, 1996; *Anderson et al.*, 1998a, 1998b; *Schröder et al.*, 1998, 2000]. (We use the term "apparent emission index" because the particles are not directly emitted, but are formed in the plume as a function of time and thermodynamic and chemical conditions.)

4. The fraction (η^*) of fuel S apparently converted to SO_3 and small, volatile particles has been determined from in-flight measurements using a variety of techniques. The scatter in the derived value of η^* is very large [*Kawa*, 1999; *Penner et al.*, 1999]. This scatter may be due to the following: differences among techniques in the smallest size particle that can be measured; differing aircraft engines, operating conditions, and fuel S contents; the presence or absence of contrails; the varying response time of the different techniques; poorly understood instrument response as a function of particle size and concentration and operating pressure; and experimental precision and bias. The best quantified measurements and analyses suggest values for η^* from 1-31% behind a variety of military and commercial engines [*Curtius et al.*, 1998; *Miake-Lye et al.*, 1998; *Anderson et al.*, 1998a; *Schröder et al.*, 1998; *Kärcher et al.*, 1998a, 1998b].

5. The rapid formation and growth of small sulfate particles in aircraft plumes that has been observed cannot be accounted for by classical binary, homogenous nucleation, and collisional growth in numerical models. Instead, chemi-ions emitted by the engine are thought to promote the nucleation and coagulation of charged molecular clusters to produce stable, initially charged particles [*Yu and Turco*, 1997, 1998a; *Kärcher et al.*, 1998a, 1998b]. The number EI* of particles in this charged "ion mode" is believed to be controlled by these chemi-ion emissions, while the size of the ion mode particles is likely controlled by the FSC. A second, neutral mode of particles formed by classical homogeneous nucleation and controlled in number by the FSC is also believed to be present in the exhaust plume, but may be too small to be detectable at typical FSCs. The presence of chemi-ions in aircraft engine exhaust has been been documented; however, measurements of chemi-ion concentrations and properties both on the ground and in flight are very sparse and represent lower limits [*Arnold et al.*, 1998a, 1998b, 1999].

6. At low values of FSC it has been hypothesized that nonmethane hydrocarbons (NMHCs) may contribute significantly to the formation and mass of small, volatile particles [*Kärcher et al.*, 1998a]. Thus, even at zero FSC, significant number EI^*s of particles may still result, and values of η^* calculated assuming a composition of H_2SO_4/H_2O may be biased high.

In this work, we present and evaluate measurements of particle size distributions made behind a Boeing B737-300 aircraft in flight during the Sulfur-6 experiment. The goals of this work are as follows: to report the first fast-response measurements of highly resolved particle size distributions of the small, volatile particles produced in aircraft plumes; to carefully document the experimental uncertainties and conditions under which the measurements were made; to use these measurements to provide estimates of the number, surface, and volume EI^*s and of η for fuels with very low FSC; and to discuss the implications of these observations. An overview of the Sulfur-6 experiment and volatile particle number EI^*s is given by *Schröder et al.* [2000], while *Petzold et al.* [1999] discuss the emissions of carbon soot measured during this and other experiments.

2. Experimental Technique

2.1. Experimental Configuration and Calibration

Measurements of particle concentration were made using nine particle counters operating in parallel. These instruments, condensation nucleus counters (CNCs), detect and count particles larger than a minimum size by condensing a working fluid (usually n-butyl alcohol) on the small particles and growing them to droplets that are easily counted [e.g., *Stolzenburg and McMurry*, 1991]. The minimum detectable diameter is controlled by the supersaturation and growth time within the condenser of the instrument. The supersaturation and growth times may be controlled by varying the geometry, temperature, and/or flow rate of the condenser and/or by changing the working fluid. Each of the CNCs used in this study operated with a different supersaturation by adjusting these parameters, and thus had different minimum detectable diameters.

Five of the CNCs were housed in a single instrument, the University of Denver's nucleation-mode aerosol size spectrometer (N-MASS) (C. A. Brock, manuscript in preparation, 2000). The five CNCs within this instrument operate in parallel at a fixed pressure of 60 hPa. The sample

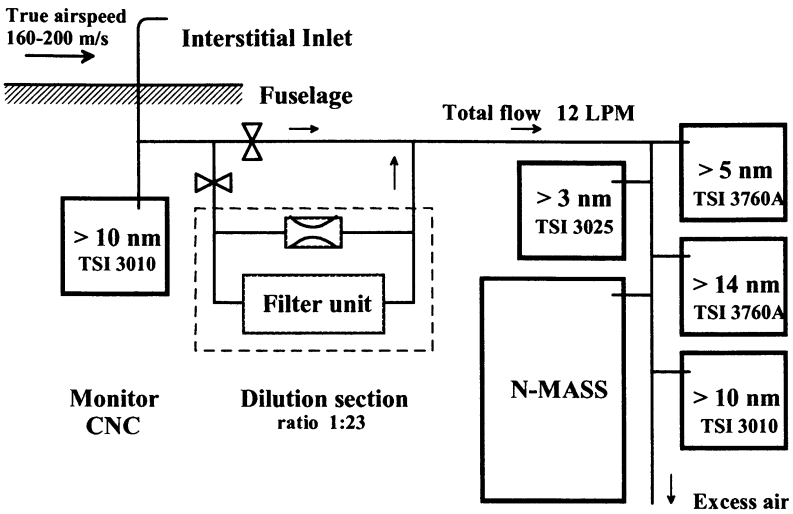

Figure 1. Schematic of the aerosol sampling system used aboard the Falcon during Sulfur-6 [*Schröder et al.*, 2000]. The backward oriented interstitial sampling inlet is mounted on top of the cabin, approximately 3 m behind the cockpit and about 35 cm from the fuselage. After passing (an optional) dilution section (ratio 1:(23±4)) the aerosol sample is transported to the CNCC and the N-MASS systems.

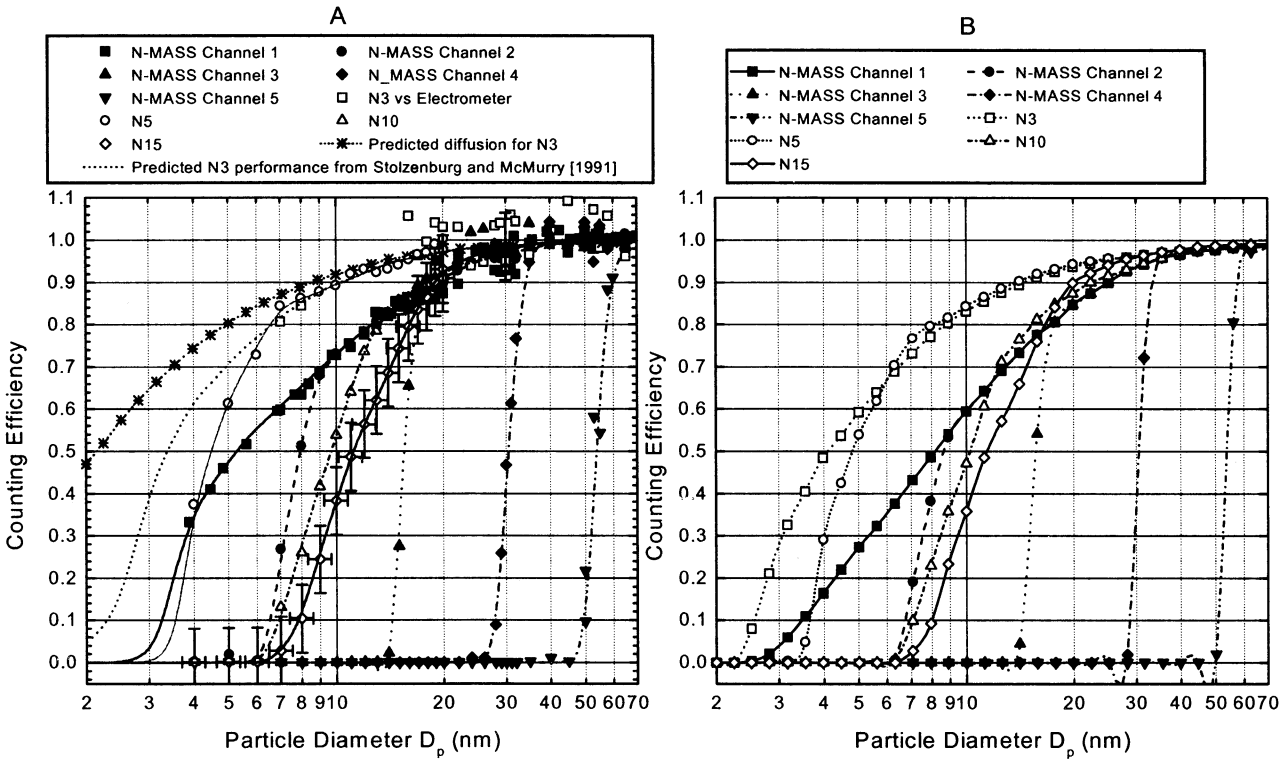

Figure 2. (a) Measured detection efficiency of the DLR CNCs (N5, N10, and N15) and the five channels of the University of Denver N-MASS, using the aircraft tubing system, as a function of particle diameter D_p at a pressure of 960 hPa, relative to the N3 instrument (a TSI 3025A). A representative experimental calibration uncertainty is demonstrated by the error bars on the N15 instrument. The points are experimental data, and the lines are fits to the data. Points for the N3 (TSI 3025A, the reference instrument) are relative to an electrometer. Calculated diffusion losses within the tubing leading to the N3 instrument are shown, as is a calibration for this instrument (with diffusion losses added) as determined by *Stolzenburg and McMurry* [1991], which extends to smaller sizes than we achieved in our experimental configuration. The calibration aerosol is composed of $(NH_4)_2SO_4$. (b) Calculated response of the instruments at 321 hPa operating pressure, based on the fitted curves in Figure 2a and calculated diffusion losses within the sampling system at the measurement pressure.

airstream flows through a critical orifice into a sampling chamber that follows the design of *Pui et al.* [1990] to minimize particle losses. The remaining four CNCs, operated by DLR, were placed in parallel with the N-MASS sampling continuously from a single, rear-facing inlet (Figure 1). This inlet has been characterized in flight [*Schröder and Ström*, 1997] and found to transmit particles with diameters >500 nm with poor efficiency, so that contrail ice crystals are not directly sampled. Since impact shattering of ice crystals have been found to produce only a small effect on CN concentrations for forward facing inlets [*Weber et al.*, 1998], it is unlikely that a significant sampling artifact exists for our rear-facing inlet within contrails. After entering the aircraft, the very high concentration sample flow was diluted by a ratio of 1:(23±4) with filtered ambient air. The instruments exhausted to a venturi exit, and were operated internally at a measured pressure slightly lower than the ambient value. Convective heat transfer between the aircraft cabin and the sampling tubing resulted in an estimated heating of the sample flow to near cabin temperature. The instrument package was installed on a Dassault Falcon 20, an small twin-engine jet aircraft operated by DLR from Oberpfaffenhofen, Germany.

Immediately following the measurements, the particle instrument package was calibrated in the laboratory (Figure 2). Particles of $(NH_4)_2SO_4$ were produced by condensation following heating of the solid in a flowing tube furnace. The particles were classified in a differential mobility analyzer (DMA, Model 3071A, TSI, Inc., St. Paul, Minnesota, United States) to produce a nearly monodisperse, singly charged, calibration aerosol. This calibration aerosol was diluted and introduced simultaneously into the aircraft sampling tubing and into a Faraday cup attached to an electrometer. The electrometer provides a fundamental measurement of the concentration of particles produced by the DMA. However, because a relatively high concentration of particles was required to produce a significant signal on the electrometer, it was not used as the primary calibration reference. Instead, a TSI Model 3025A CNC, which was part of the flight package, was used as the standard against which the other instruments were calibrated. Over a range of particle sizes from 6 to 60 nm, the ultrafine particle counter and the electrometer agreed linearly to within 2% following corrections to the TSI data for diffusion losses and particle-in-beam coincidence (Figure 3). Calibration particles with diameters $D_p < 4$ nm could not be produced; the calibration curves for smaller diameters are extrapolated (for N-MASS channel 1 and N5) or based on published data (for N3, see *Stolzenburg and McMurry* [1991]).

The calibration of the nine CNCs shows sharp cutoff characteristics for particles with D_p greater than about 13 nm, and more gradually sloping curves for particles with smaller D_p. This sloping response is due to substantial diffusion losses in the sampling tubing and, particularly for the N-MASS for $D_p < 10$ nm, within the instruments themselves. Diffusion losses in incompressible, fully developed, laminar pipe flow are readily calculated [*Gormley and Kennedy*, 1949]. Diffusion losses increase as pressure decreases. On the basis of the measured tubing lengths and known volumetric flows of the instruments, diffusion losses in the sampling lines have been calculated as a function of D_p for the calibration pressure (960 hPa) and the three principal in-flight sampling pressures (approximately 450 , 320, and 205 hPa inside the instruments). These diffusion losses have been

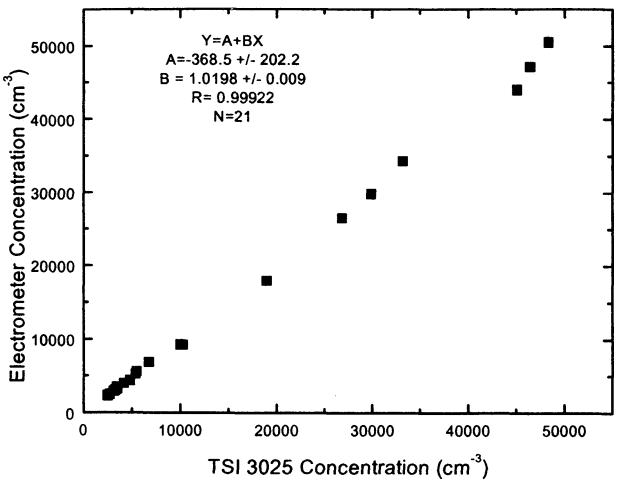

Figure 3. Counting efficiency of the TSI Model 3025 CNC used as the calibration reference standard as established against the primary standard, a Faraday cup and electrometer.

incorporated into the algorithm used to calculate the size distribution from the CNC measurements, as described below. We note that the diffusion calculations do not account for losses in the tubing bends, where radial velocity components can increase diffusional deposition to the walls. Particle losses due to inertial deposition are negligible for the D_p (<50 nm) considered here and the flowrates and radii of curvature in the sampling tubes.

The calibration shown in Figure 2 is for an aerosol composed of $(NH_4)_2SO_4$. There is evidence of a shift in the response function of the CNCs that use n-butyl alcohol as the working fluid when the calibration aerosol is composed of NaCl instead of $(NH_4)_2SO_4$. [*Schröder et al.*, 2000; *Saros et al.*, 1996]. The N-MASS, which uses perfluoro-tributylamine $(CF_3(CF_2)_3)_3N$), an hydrophobic, relatively inert compound, as the working fluid, has not shown a detectable sensitivity to particle composition in laboratory tests with NaCl, $(NH_4)_2SO_4$, H_2SO_4, and Ag particles. For the butanol-based CNCs, however, differences in the instrumental response between the laboratory calibration aerosol and the aircraft-produced particles remain a potential bias.

An interesting feature in Figure 2 is the crossing of the N-MASS channel 1 response curve with the N5 counter at $D_p <$ 4 nm. Given this response, one might expect that a particle number distribution heavily weighted toward particle with D_p > 4 nm would produce higher concentrations on the N5 counter relative to the N-MASS channel 1 counter, while a particle number distribution weighted toward particles with $D_p < 4$ nm would cause the N-MASS channel 1 counter to exceed the N5 counter. A transition between these two cases is indeed seen in the data (Figure 4), where ambient, extraplume size distributions were dominated by particles with $D_p > 5$ nm, while in-plume size distributions were weighted toward smaller particles. These observations improves confidence in the crossing of the response curves in Figure 2, which is based largely on extrapolation of calibration data for $D_p < 4$ nm.

2.2. Method to Determine the Particle Size Distribution

From the measurements of concentration from the multiple parallel CNCs used in Sulfur-6, we wish to determine the size

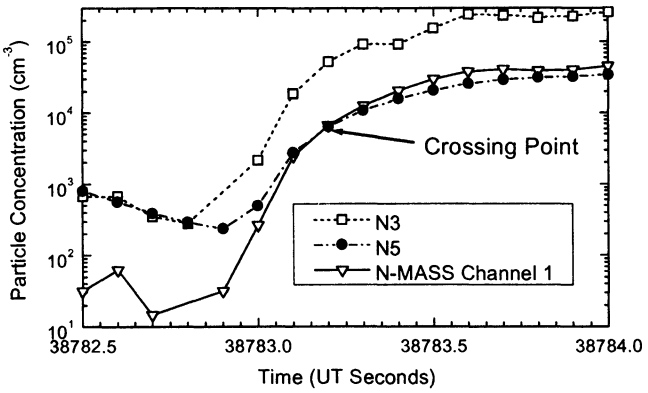

Figure 4. Concentration of particles measured at 10 Hz by the N3 and N5 channels of the DLR CNCs and the first channel of the N-MASS. The edge of a plume occurs at 38783.0 s. Prior to entering the plume, the concentration measured by N5 exceeded that measured by N-MASS channel 1. Inside the plume, N5 was less than N-MASS channel 1. This transition is caused by a shift in the size distribution from a peak at $D_p > 4$ nm to a peak at $D_p < 4$ nm (see Figure 2 and text).

distribution of particles in the plumes of flying aircraft. These size distributions can be used to calculate the number, surface area, and volume concentration of particles within a given size range, which can then be related to the S content of the fuel and other controlling parameters. One approach that has been used in the past to determine differential size distributions [e.g., *Schröder et al.*, 2000] is to subtract the concentrations of adjacent CNCs, and assign the resulting concentration to the size interval lying between the nominal 50% size cut diameters of the CNCs. For the data presented here, this method can be used quantitatively only for particles with $D_p > 12$ nm [*Petzold et al.*, 1999]. For smaller particle diameters, the sloping, and even crossing, response functions argue against such an approach.

An alternative method, used here, is to make use of an inversion technique to determine a smooth, nonnegative particle size distribution function that is consistent with the responses measured simultaneously by the parallel CNCs. Each of the CNCs i records a single number X_i,

$$X_i = \int_0^\infty N(D_p) K_i(D_p)\, dD_p, \qquad (1)$$

where N is the particle size distribution function (the number of particles occurring between particle diameters D_p and $D_p + dD_p$) and $K_i(D_p)$ is the response function of instrument i to a particle of size D_p (Figure 2). Note that the $K_i(D_p)$ vary as a function of pressure due to changing diffusion losses in the sampling system. The inverse problem is, given $K_i(D_p)$ known with experimentally characterized uncertainty, and X_i measured with known uncertainty, what is $N(D_p)$? We solve a finite difference approximation of (1) for $N(D_p)$ using a version of the smoothed Twomey (ST) algorithm [*Markowski*, 1988]. This constrained nonlinear inversion technique is used to generate a 33-point representation of $N(D_p)$ for $2 \le D_p \le 80$ nm. An infinite number of possible $N(D_p)$ that satisfy (1) exist, most of which are characterized by oscillations on scales smaller than the diameter difference between adjacent CNC channels. The ST method uses a nonlinear technique to choose one smooth, nonnegative solution that does not contain these high frequency modes by minimizing, to within experimental uncertainty, a chi-squared value related to the difference between the predicted and actual instrument response through an iterative weighting and smoothing scheme. The algorithm accounts for the sloping, crossing nature of the response functions and produces a size distribution that is consistent with the concentrations measured by each CNC. Variants of the smoothed-Twomey algorithm have been used to recover size distributions from diffusion batteries [*Markowski*, 1988], impactors [*Winklmayr et al.*, 1990], optical particle counters [*Jonsson et al.*, 1995], and differential mobility analyzers (D. Collins et al., Improved inversion of scanning DMA data, submitted to *Journal of Geophysical Research*, 2000).

Table 1. Sources of Random (Class R), Systematic (Class=S) and Numerical (Class=N) Uncertainties in Determining Particle Number EI*

Class	Source	Estimated Magnitude	Comments
R	instrument flow uncertainty	8%	see calibration scatter (Figure 2)
R	calibration reference	5%	electrometer and N3 uncertainties
R	counting statistics	<1% N3 <10% N-MASS channel 5	good statistics in plumes
R	plume dilution	12%	dilution calculated from CO_2
R	plume integration	20%	
R	sample dilution	15%	
R	linear propagation of above random errors	28%	for dilution and integration only; other errors accounted for in Monte Carlo simulation
S	inertial segregation at sampling inlet	± 5%	small error for $D_p < 50$ nm; see *Schröder et al.* [1998]
S	enhanced diffusion losses in tubing bends	- 5%	small fraction of total diffusion losses
S	extrapolation of calibration curves	± 50%	significant possible bias at very small particle sizes; sign of bias unknown
N	choice of smoothing parameter and propagation of other uncertainties in inversion	±26%	calculated for $D_p < 10$ nm only first three random uncertainties listed above (which apply randomly to each channel) are considered

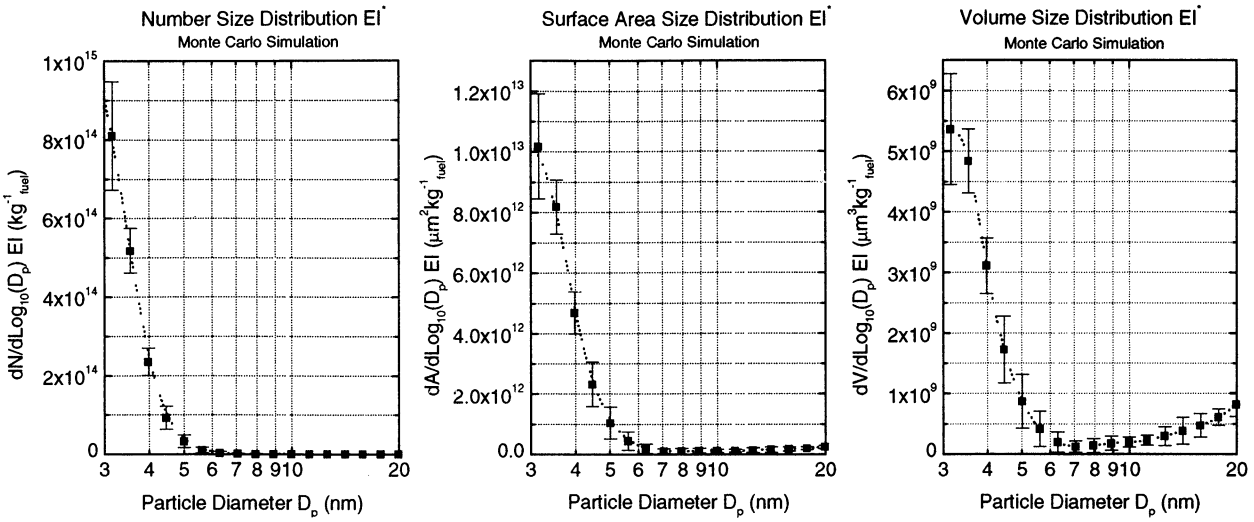

Figure 5. Results of a 100-iteration Monte Carlo simulation of the propagation of the first three random (class R) experimental uncertainties in Table 1 for a particle volume size distribution (volume of particles per size increment per kilogram of fuel burned). Points show the median and range of solutions. Original data are from in-flight measurements in an aircraft plume.

2.3. Analysis of Uncertainties

We have identified three primary sources of uncertainty in the measurements and analysis. These uncertainties are summarized in Table 1. The first of these is a random uncertainty due to the precision of the measurement of particle emission indices. This uncertainty stems from measurement precision of the particle concentrations measured by the multiple CNCs (which are dominated by flow uncertainties and counting statistics), uncertainty in integrating the measurements over a fixed time period in the plume, uncertainty in determining the FSC, and uncertainty in determining the dilution factor within the plume based on CO_2 and/or temperature measurements.

The second type of uncertainty includes possible systematic errors, such as sampling biases due to inertial segregation at the rear-facing sampling inlet, improper estimation of diffusional losses in curved tubing, and errors in the response curves of the CNCs due to extrapolation of calibration data for $D_p < 4$ nm.

The third source of uncertainty stems from the inversion algorithm applied to determine the particle size distribution function. A user-defined smoothing parameter is used to limit high-frequency oscillations of the solution. This smoothing parameter has been chosen based on laboratory studies using the five-channel N-MASS and a scanning mobility particle sizer. To constrain the uncertainty introduced by this choice of smoothing parameter, and to evaluate how experimental precisions propagate through the data inversion, we have performed a Monte Carlo sensitivity test (Figure 5 and Table 2). This analysis excludes the possible biases noted in Table 1.

3. Results

The goal of this study is to evaluate the apparent emission indices (EI^*) of aerosol particle number, surface, and volume as produced by aircraft and engines representative of the commercial subsonic fleet. To this end, we will focus on a subset of the Sulfur-6 data that relates to the emissions from a Lufthansa B737-300 with CFM56-3B1 engines flying at normal operating speeds at flight level (FL) 190, 260, and 350-370 (5.8, 7.9, and 10.7-11.3 km above sea level, respectively). The aircraft was supplied with fuel with a FSC of only 0.8 ppmm as measured at the source. Following transport in a tanker truck, fueling of the aircraft and flight, a sample taken from the aircraft tank contained a FSC of 2.6 ± 0.3 ppmm FSC. Fuel containing 56 ± 6 ppmm FSC was flown in another fuel bladder on the aircraft. In flight each engine could be operated from either fuel source independently or simultaneously, a concept first executed by *Busen and Schumann* [1995].

An overview of the flight and of particle number EI*s appears in the work of *Schröder et al.* [2000]. In this paper, we will examine size distributions measured in the following cases in detail:

1. The first case is approximately 0.3-0.4 s after emission at FL190 (5.8 km) in a humid, but non-contrail-forming, environment when the B737-300 was burning 56 ppmm and 2.6 ppmm FSC fuel simultaneously on different engines.
2. The second case is from 0.2 to 0.6 s after emission at FL260 (7.9 km) under relatively dry conditions while the aircraft burned 56 ppmm and 2.6 ppmm FSC fuel simultaneously on different engines. We will examine the change in particle size distribution as a function of plume age in this case.

Table 2. Propagation of Total Random Uncertainties, Including Numerical Uncertainties (Table 1), to the Final Number, Surface and Volume EI^* and η^* Data Products

Parameter	Magnitude of Uncertainty, %
number EI^*	38%
surface EI^*	36%
volume EI^*	36%
η^*	36%[a]

[a]Includes 11% uncertainty in determining fuel sulfur content at 2.6 ppmm.

Table 3. Meteorological and Aircraft Parameters

Case	Flight Level, hundreds of feet, km	Pressure, hPa	Temperature, °C	True Airspeed, m s^{-1}	Engine Speed, %	Fuel Flow, kg h^{-1} $engine^{-1}$
1	FL190, 5.8	490	-14	141	72	1000
2	FL260, 7.9	360	-30	167	72	750
3	FL350, 10.7	235	-52	192	79	770-800
4	FL370, 11.3	215	-56	199	79	730

3. The third case is from 0.3 to 0.6 s after emission at FL350 (10.7 km) in contrail-forming conditions as the aircraft burned 2.6 ppmm FSC fuel.

4. The fourth case is approximately 20-30 s after emission in a dissipating contrail at FL370 (11.3 km) as the aircraft burned 2.6 ppmm FSC fuel.

Information on atmospheric temperature and pressure and on aircraft technical parameters for each of the four cases are given in Table 3. The results of the particle measurements are summarized in Table 4.

3.1. Case 1: High S/Low S, Low Altitude, Humid, No Contrail

At FL190 (5.8 km), measurements were made behind the left and right engines, which were burning fuels with different FSCs. The plumes behind each engine were penetrated multiple times. Size distributions were derived from the CN concentrations as measured at about 85 m behind the B737-300, or approximately 0.5 s after emission, by averaging over the densest portion of the plume. Dilution factors and EIs were determined as described in detail by *Schröder et al.* [2000]. Plume ages of less than 1 s were determined from triangulation of cockpit videotape data corrected for the initial velocity of the aircraft exhaust and are accurate to within 10%.

Differential number, surface area, and volume size distributions (Figure 6), which are commonly expressed in units of quantity per cubic centimeter of air per logarithmic size interval, are shown here as quantity per kilogram of fuel burned per logarithmic size interval. This unusual scaling eliminates the effects of variable dilution factors, and places the size distributions in a format that can be readily used in atmospheric models that incorporate aircraft fuel usage. We will restrict the discussion of the size distributions to particles with D_p<10 nm and exclude larger, soot-influenced modes [*Petzold et al., 1999*]. The size distributions tend to peak near the minimum detectable diameter of the particle counters used to derive the distributions. At the low FSCs used in Sulfur-6, the instruments are not capable of fully measuring the number distribution (the particles are too small), and some of the shape of the distribution at and below 3 nm is controlled by extrapolation within the inversion algorithm. Because these particles do not dominate the volume distribution from which mass is calculated, uncertainties induced by the extrapolation are adequately accounted for in the error propagation study shown in Figure 5 and Table 2.

The integrated EI^*s for 3 nm ≤ D_p ≤ 10 nm (Figure 6) show that the number, surface area, and mass EI^*s for the 56 ppmm FSC case are all significantly higher than for the 2.6 ppmm case. In contrast, there is no significant shift in particle diameter between the two cases for any of the weightings. The mass EI^* does not increases proportionally with the ~20x increase in FSC. Assuming that the particles are composed of H_2SO_4 solution droplets at <5% relative humidity as detected within the particle counters, the fraction of fuel S converted to particulate S, η^*, has been calculated (the asterisk indicates the compositional assumption). For the 2.6 ppmm FSC case, η^* is 17±6 %. For the 56 ppmm FSC case, η^* is 2.4 ± 0.9%. As discussed below, the higher value for the very low FSC case may indicate that other compounds, such as condensed NMHCs, contribute significantly to particle mass as FSC approaches zero. Since typical commercial jet-A fuel contains 400-600 ppmm FSC [*Penner et al.*, 1999], the value of η^*=2.4% for the 56 ppmm FSC case is more representative for the commercial aircraft fleet than is the value for the 2.6 ppmm case, although still the FSC is still quite low. We recall that these values of η^* still represent lower bounds because we cannot account for the mass fraction residing in particles below 3 nm. According to models [*Kärcher et al.*, 1998a], the mass fraction in this neutral particle mode decreases with increasing plume age and rapidly adds to the

Table 4. Summary of Observations of Apparent Number, Surface, and Volume Emission Indices (EI^*s) and Fraction of Fuel Sulfur Converted into Particulate Mass η^* Assuming a Composition of H_2SO_4/H_2O[a]

Plume Age, s	FSC, ppmm	Altitude, km	Contrail Present	Number EI^*, kg^{-1}_{fuel}	Surface EI^*, $\mu m^2\ kg^{-1}_{fuel}$	Volume EI^*, $\mu m^3\ kg^{-1}_{fuel}$	η^*, %
0.4	2.6	5.8	no	3.8×10^{16}	1.3×10^{12}	7.4×10^{8}	17
0.4	56	5.8	no	1.2×10^{17}	3.9×10^{12}	2.2×10^{9}	2.4
0.2	2.6	7.9	no	1.9×10^{16}	6.2×10^{11}	3.5×10^{8}	8.1
0.4	2.6	7.9	no	3.1×10^{16}	1.0×10^{12}	6.0×10^{8}	14
0.6	2.6	7.9	no	4.6×10^{16}	1.6×10^{12}	9.1×10^{8}	21
0.4	56	7.9	no	5.6×10^{16}	1.9×10^{12}	1.1×10^{9}	1.2
0.3	2.6	10.7	yes	1.3×10^{16}	4.7×10^{11}	2.3×10^{8}	5.2
0.4	2.6	10.7	yes	1.5×10^{16}	5.0×10^{11}	2.2×10^{8}	5.0
0.6	2.6	10.7	yes	1.6×10^{16}	5.3×10^{11}	2.3×10^{8}	5.2
20	2.6	11.3	dissipating	1.6×10^{16}	7.4×10^{11}	4.3×10^{8}	9.9

[a]FSC is fuel sulfur content. Uncertainties for the final four columns are ±38%, ±36%, ±36%, and ±38%, respectively. Arranged by altitude and FSC.

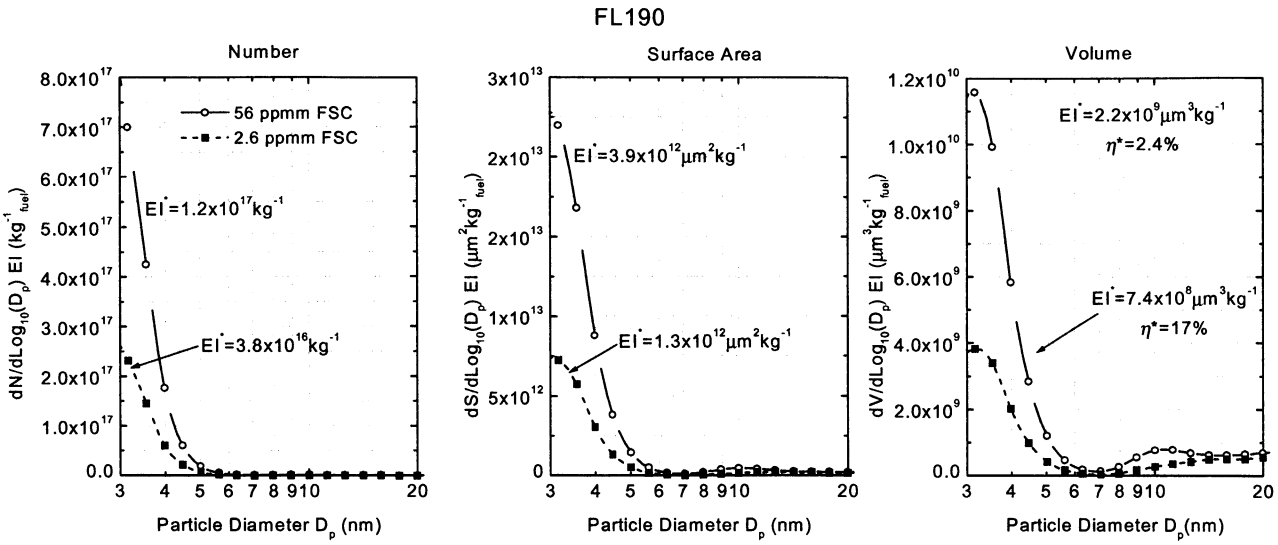

Figure 6. Differential number, surface area, and volume particle size distribution EI* determined from numerical inversion of the concentrations measured with nine CNCs aat bout 0.4 s plume age behind a B737-300 at FL190 (5.8 km). Units are in differential value per kilogram of fuel burned. The scaling of the ordinate is linear, so that an integral under the curve is the EI* of that parameter over the integrated size range. Note that a significant portion of the EI*s appears to fall in particles with $D_p < 3$ nm, the minimum detectable diameter of the CNCs. The integral values shown numerically on the graph were integrated between 2.8 and 10 nm.

mass of the detectable particles, especially for high FSCs; see also discussion of case 2.

3.2. Case 2: High S/Low S, Midaltitude, No Contrail

At FL260 (7.9 km) and a plume age of 0.4 s, a clear difference in particle number, surface area, and volume EI*s was seen between the left engine, which was burning 2.6 ppmm fuel, and the right engine, which was burning 56 ppmm fuel (Figure 7). For the 56 ppmm fuel, the number, surface, and volume EI*s were lower at this altitude than at FL190 (5.8 km) by a factor of about 2, which is statistically significant. For 2.6 ppmm they were lower by a factor of 1.2 to 1.3, which is within the uncertainty in the measurements. Possible contributors to the differences in EI* between the two altitudes for the 56 ppmm case may include ambient temperature and different engine conditions at the two altitudes (Table 3), causing possible differences in sulfur oxidation efficiency in the engine and in sulfuric acid particle nucleation and growth rates. The lack of a significant change in the 2.6 ppmm EI* s between the FL190 (5.8 km) case and

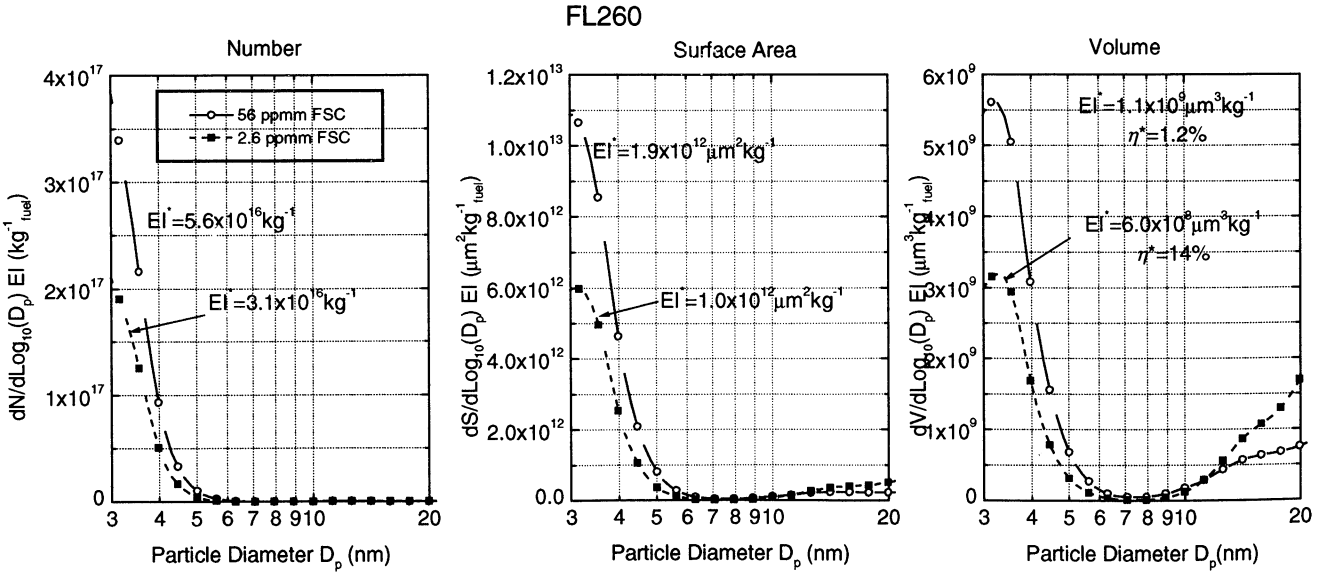

Figure 7. As for Figure 6, but for measurements made at FL 260 (7.9 km) at approximately 0.4 s plume age as the aircraft burned fuel with 2.6 ppmm FSC on the left engine and 56 ppmm FSC on the right.

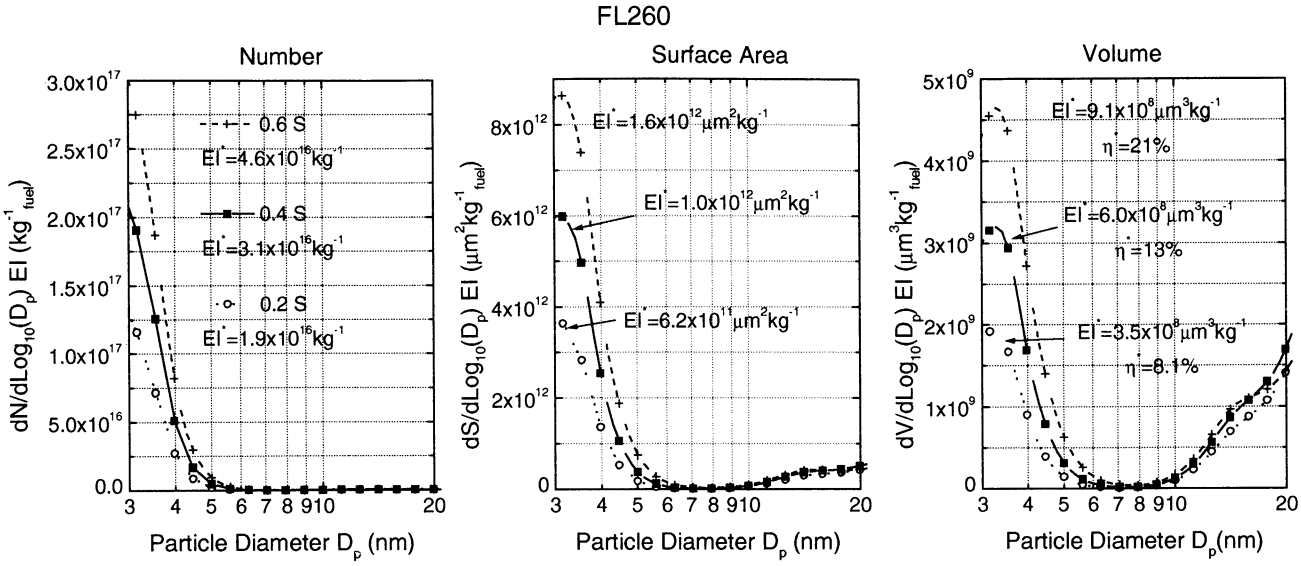

Figure 8. As for Figure 6, but measured as the aircraft burned fuel with 2.6 ppmm FSC at three different plume ages.

the FL260 (7.9 km) case suggests that most of the number, surface area, and volume of particles produced for the 2.6 ppmm case may not be composed of sulfuric acid/water droplets.

An approach from 120 to 35 m behind the B737-300 at FL260 (7.9 km) as the aircraft used fuel with a FSC of 2.6 ppmm allowed the change in particle size distribution as a function of plume age to be measured. The measured size distributions were segregated by plume age into 0.01 s age increments. The results for 0.2, 0.4, and 0.6 s plume age illustrate the growth of particle number, surface area, and volume EI* as a function of plume age (Figure 8). Particle size distributions at older plume ages could not be measured because the Falcon was unable to fly in the region between 120 m and ~3 km behind the B737 aircraft due to difficulties controlling the smaller aircraft in the rollup region of the B737 wingtip vortices. The increase in EI*s with increasing plume age occurred even for the low, 2.6 ppmm FSC, and is qualitatively similar to the growth modeled behind the DLR ATTAS aircraft burning fuel with FSC=20 ppmm [*Yu et al.*, 1998; *Schröder et al.*, 2000]. On the basis of this dependence of the observed number EI*s with plume age, the values for the number EI*s presented here will likely increase by a factor of ~2-3 at older plume ages as particles grow into sizes that can be detected by the CNCs. The surface and mass EI*s should also increase, but by a slightly lesser amount.

3.3. Case 3: Low S, High Altitude, Young Contrail

At FL350 (10.7 km), ambient thermodynamic conditions were such that a contrail was formed within a few meters of the exhaust plane of each engine of the B737. These contrails

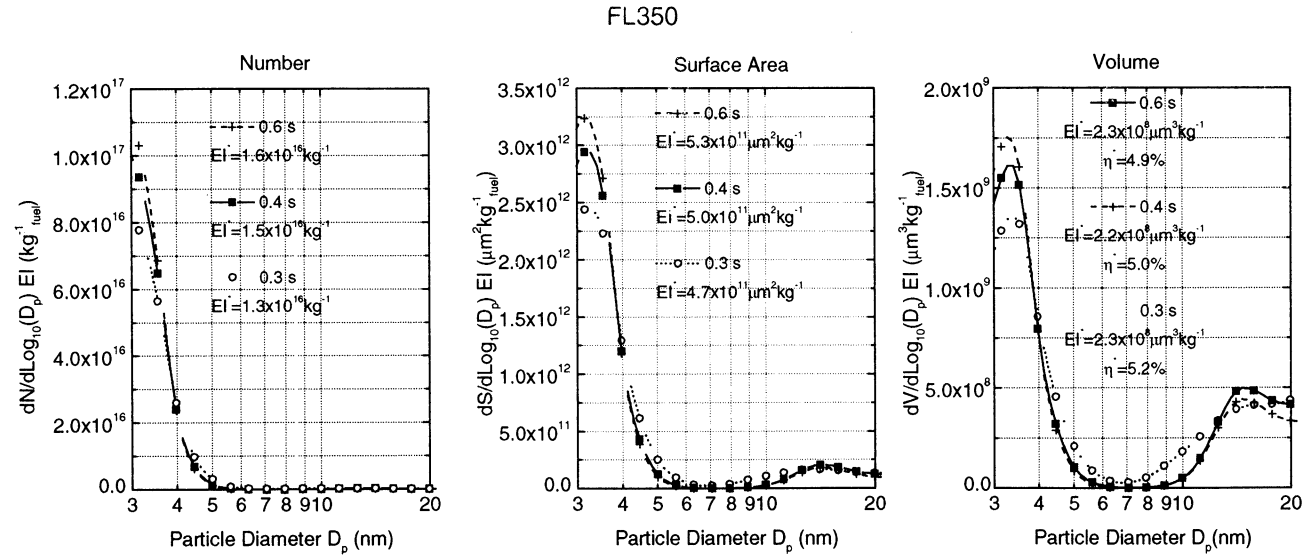

Figure 9. As for Figure 6, but measured as the aircraft burned fuel with 2.6 ppmm FSC at three different plume ages while measuring in a newly formed contrail.

persisted for at least several tens of seconds, or several kilometers distance. Measurements were made both in the near field wake of the contrailing aircraft, and 3-4 km after emissions where the dissipating, but still visible, contrail could be penetrated. In the near-field environment, measurements were made as the Falcon approached the B737 from 140 to 70 m behind the engine, or plume ages of 0.6 to 0.3 s, using the rear-facing aerosol inlet that effectively excludes contrail particles from the sample stream. Particle size distributions determined from the multiple CN counters show only slight changes in the interstitial aerosol as a function of plume age (Figure 9). The differences in integral number, surface, and volume EI*s are not significant given the experimental uncertainties summarized in Table 2. This behavior is in marked contrast with the results from FL260 (7.9 km), which showed a strong increase in EI*s for number, surface, and volume. Number EI*s were lower by a factor of ~3 for the 0.6-s-old plume in the contrail case compared with the lower-altitude, noncontrail case. As discussed by *Kärcher* [1999] and *Schröder et al.* [2000], this significant decrease in particle number EI* is likely caused by diffusional coagulation of small particles to the ice surface.

3.4. Case 4: High S/Low S, High Altitude, Evaporating Contrail

Measurements were also made at FL370 (11.3 km) in the contrail at an age of ~20 s, or 4 km behind the B737 aircraft. At this stage the contrail was beginning to dissipate, becoming wispy and diffuse. Measurements of the interstitial aerosol (Figure 10) show number EI*s that were within measurement uncertainty of the in-contrail values at plume ages ≤ 0.6 s. In other words, no net particle formation occurred between the early stages of the contrail lifetime and the dissipating stage of the contrail. Particle surface area EI* appeared to increase with contrail age, although this increase was within measurement uncertainty, while particle volume EI* increased significantly. The increased particle volume is probably associated with the growth of particles that were not incorporated into the contrail crystals, since the residue from evaporating crystals would likely be larger than 10 nm.

4. Discussion

A critical parameter in estimating the effect of a future supersonic aircraft fleet on the stratosphere is the fraction of fuel S that rapidly forms small particles, η^* [*Fahey et al.*, 1995; *Kawa*, 1999; *Weisenstein et al.*, 1998]. If a significant fraction of aircraft S emissions result in the formation of many small particles rather than gradual oxidation of emitted SO_2 by OH and subsequent condensation onto preexisting particles, stratospheric aerosol surface areas are increased. For values of η^* of 0%, 10%, 50%, and 100%, the modeled increase in background stratospheric surface area concentration for a scenario with a 500-aircraft supersonic fleet is 27%, 38%, 82%, and 111%, respectively [*Kawa*, 1999]. This modification to the stratospheric aerosol surface area strongly affects stratospheric ozone by perturbing the NO_x, HO_x and ClO_x budgets, mostly by repartitioning the odd nitrogen budget via N_2O_5 hydrolysis.

In light of the calculated sensitivity of stratospheric chemistry to possible future aircraft emissions, in particular the value of η^*, it is useful to review the extant literature reporting measurements of this parameter (Table 5). Of the measurements listed in Table 5, several do not provide adequate detail of experimental conditions, techniques, and uncertainties to evaluate the total uncertainty in the derivation of η^* from the measurements. Several cases do not indicate if a contrail was present or absent, or the age of the plume at the time of the measurement. As a consequence of these variations in experimental capability and circumstance, reported values of η^* range from 0.34% to 55%.

The measurements reported here, showing values of η^* of a few percent for the 56 ppmm case and ~10-20% for the 2.6 ppmm case, can be compared with those in Table 5 that are well characterized, reporting experimental uncertainties and sampling circumstances. (Remember that the values we determined would likely have increased by ~2-3 times for older plume ages than we could sample.) The values we report are somewhat lower than those determined by *Anderson et al.* [1998a] and *Miake-Lye et al.* [1998] behind a Boeing 757 burning fuel with a FSC of 72 ppmm, and are generally consistent with the ATTAS observations and

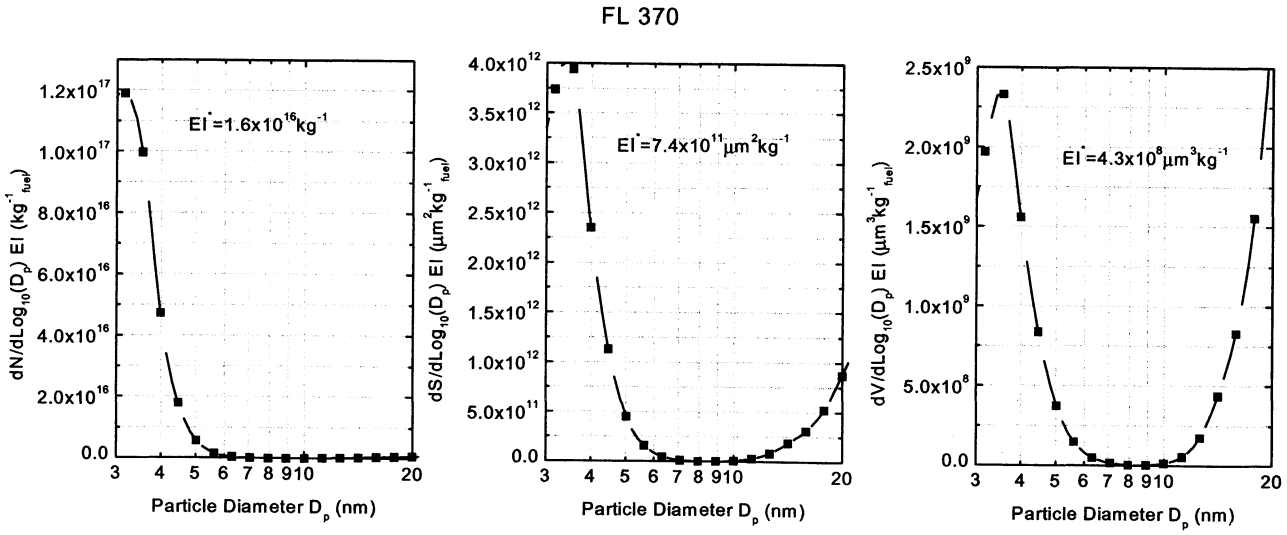

Figure 10. As for Figure 6, but measured as the aircraft burned fuel with 2.6 ppmm FSC at a plume age of ~20 s in a dissipating contrail.

Table 5. Volatile Particle Number EI and Fraction η^* of Fuel S Converted to Particulate Sulfate or Condensable S Compounds, Measured in the Exhaust of Aircraft in Flight[a]

Number EI, kg^{-1}_{fuel}	η^*, fraction of fuel S converted to particles (or S(VI)) for CIMS	Technique	Aircraft	Engines	Flight Conditions	Fuel S Content, ppmm	Reference
$5\text{-}20\times10^{15}$	0.55	CNC/ model	DLR ATTAS		varied	20	*Schröder et al.* [1998] *Kärcher et al.* [1998b]
$\sim2\times10^{15}$	>0.08 (±0.03)	CNC	NASA 757	RB211	varied	72	*Miake-Lye et al.* [1998]
	0.06 (0.0-0.34)	CIMS	NASA 757	RB211	varied	72	*Miake-Lye et al.* [1998]
	0.37	impactor/ electron microscopy	NASA 757	RB211	varied	72	*Pueschel et al.* [1998]
$2.1(\pm0.3)\times10^{14}$	0.11	DMA	NASA 757	RB211	varied	72	*Hagen et al.* [1998]
$1.7\text{-}6.5\times10^{17}$	>0.12	CNC	Concorde	Olympus 593	supersonic cruise	230	*Fahey et al.* [1995]
$\sim8\times10^{16}$	>0.15 (±0.07)	CNC	NASA 757	RB211	varied	676	*Miake-Lye et al.* [1998]
	0.31(0.16-0.52)	CIMS	NASA 757	RB211	varied	676	*Miake-Lye et al.* [1998]
$2.5(\pm0.4)\times10^{15}$	0.022	DMA	NASA 757	RB211	varied	676	*Hagen et al.* [1998]
	0.10-0.26	impactor/ electron microscopy	NASA 757	RB211	varied	676	*Pueschel et al.* [1998]
	0.0034	volatilization/ CIMS	DLR ATTAS		varied	2700	*Curtius et al.* [1998]
$\sim1\text{-}2\times10^{17}$	0.018	CNC	DLR ATTAS		varied	2700	*Schröder et al.* [1998] *Kärcher et al.* [1998a]

[a]Volatile particles are presumed to be composed of H_2SO_4/H_2O. Arranged by increasing FSC.

modeling by *Schröder et al.* [1998] and *Kärcher et al.* [1998]. (Note that the observations reported here are not entirely independent of the Schröder et al. and Kärcher et al. work, as the same measurement platform was used with the same, rearward facing inlet, albeit with several different instruments.) Miake-Lye et al. do not state the age of the plume or the exact distance of the measurements, which makes them difficult to directly compare with the values reported here, and their measurements were taken while the B757 aircraft produced a short-lived contrail (R. C. Miake-Lye, personal communication, 1998). We note, however, that the trend in the value of η^* reported by *Miake-Lye et al.* [1998], with increasing values of η^* with increasing FSC, is in disagreement with our observations of decreasing η^* with increasing FSC.

Chemical transport models applied to estimate the effects of the current and future aircraft fleets have parameterized aircraft particulate S emissions by applying values of η^* ranging from 0% to 100% [*Kawa*, 1999; *Penner et al.*, 1999] as input. On the basis of our measurements and analysis, a value of <10%, and perhaps <5%, for η^* is representative of the current aircraft fleet. These values are in general agreement with the recommendations of *Penner et al.* [1999] and *Kawa* [1999]. However, it is important to note that the current parameterization of plume particle formation in global models does not include the effects of chemi-ions and organics on particle formation and evolution. For this reason, applying lower values of η^* in such models must be accompanied by changes to the parameterization scheme that takes into account new microphysical understanding (B. Kärcher et al., On the unification of aircraft ultrafine particle emission data, in press, *Journal of Geophysical Research*, 2000). Also, since a fundamental understanding of the processes governing the oxidation of fuel S to SO_3 in aircraft engines has not been achieved, and since future aircraft engine technologies are not established, η^* must still be parameterized with a wide range of values for estimating the atmospheric effects of future aircraft.

The detection of sub-5 nm particles even with a FSC of only 2.6 ppmm strongly suggests that nonsulfate compounds, probably NMHCs, condense in aircraft plumes. While the efficiency of S oxidation in aircraft engines is expected to increase with decreasing FSC, calculated monatomic oxygen concentrations are expected to be insufficient to oxidize more than 10-15% of the emitted SO_2 [*Brown et al.*, 1996b]. As more data are obtained at low FSCs, it appears increasingly likely that non-S species become significant contributors to the aerosol mass budget in aircraft plumes as FSC values drop below several tens of ppmm. As demonstrated by our measurements, eliminating S from aircraft fuels is unlikely to completely eliminate volatile particle formation, although surface area and volume EI*s and the atmospheric residence time of the volatile particles will decrease.

Finally, as discussed in more detail by *Schröder et al.* [2000], the observations from Sulfur6 demonstrate the same functional form of increasing particle EI* with increasing

plume age as do aircraft plume models that incorporate chemi-ion-influenced particle microphysics [e.g., *Yu and Turco*, 1997, 1998a; *Kärcher et al.*, 1998a; 1998b]. The size distributions and values of EI^* reported here should provide strong constraints to such models since they must match not only particle number EI*s, but also surface and volume EI^*s and the particle size distribution function.

Acknowledgements. We gratefully acknowledge the contributions of R. Baumann, J. Demmel, H. G. Krafczyk, H. Rüba, P. Schulte, H. Sedlmayr, U. Schumann, and the staff of the DLR Flight Department. Lufthansa graciously provided the Boeing 737-300 aircraft and pilots used in the test flights. The Sulfur-6 experiment was performed by DLR with partial support of the Bundesministerium für Bildung und Forschung (German Secretary of Education and Research, BMBF). C. Brock was supported by the NASA's Atmospheric Effects of Aviation Project under grant NAG 2-1269.

References

Anderson, B. E., W. R. Cofer, D. R. Bagwell, K. E. Brunke, J. W. Barrick, C. H. Hudgins, and G. D. Nowicki, Airborne observations of aircraft aerosol emissions, 1, Total and nonvolatile particle emission indices, *Geophys. Res. Lett.*, *25*, 1689-1692, 1998a.

Anderson, B. E., W. R. Cofer, D. R. Bagwell, K. E. Brunke, J. W. Barrick, C. H. Hudgins, and G. D. Nowicki, Airborne observations of aircraft aerosol emissions, 2, Factors controlling volatile particle production, *Geophys. Res. Lett.*, *25*, 1693-1696, 1998b.

Arnold, F., T. Stilp, R. Busen, and U. Schumann, Jet engine exhaust chemi-ion measurements: Implications for gaseous SO_3 and H_2SO_4, *Atmos. Environ.*, *32*, 3073-3077, 1998a.

Arnold, F., K.-H. Wohlfrom, M. W. Klemm, J. Schneider, K. Gollinger, U. Schumann, and R. Busen, First gaseous ion composition measurements in the exhaust plume of a jet aircraft in flight: Implications for gaseous sulfuric acid, aerosols, and chemiions, *Geophys. Res. Lett.*, *25*, 2137-2140, 1998b.

Arnold, F., J. Curtius, B. Sierau, V. Bürger, R. Busen, and U. Schumann, Detection of massive negative chemiions in the exhaust plume of a jet aircraft in flight, *Geophys. Res. Lett.*, *26*, 1577-1580, 1999.

Brown, R. C., R. C. Miake-Lye, M. R. Anderson, C. E. Kolb, and T. J. Resch, Aerosol dynamics in near-field aircraft plumes, *J. Geophys. Res.*, *101*, 22,939-22,953, 1996a.

Brown, R. C., M. R. Anderson, R. C. Miake-Lye, C. E. Kolb, A. A. Sorokin, and Y. Y. Buriko, Aircraft exhaust sulfur emissions, *Geophys. Res. Lett.*, *23*, 3603-3606, 1996b.

Busen, R., and U. Schumann, Visible contrail formation from fuels with different sulfur contents, *Geophys. Res. Lett.*, *22*, 1357-1360, 1995.

Cofer, W. R., III, B. E. Anderson, E. L. Winstead, and D. R. Bagwell, Calibration and demonstration of a condensation nuclei counting system for airborne measurements of aircraft exhausted particles, *Atmos. Environ.*, *32*, 169-177, 1997.

Curtius, J., B. Sierau, F. Arnold, R. Baumann, R. Busen, P. Schulte, and U. Schumann, First direct sulfuric acid detection in the exhaust plume of a jet aircraft in flight, *Geophys. Res. Lett.*, *25*, 923-926, 1998.

Fahey, D. W., et al., Emission measurements of the Concorde supersonic aircraft in the lower stratosphere, *Science*, *270*, 70-74, 1995.

Gierens, K., and U. Schumann, Colors of contrails from fuels with different sulfur contents, *J. Geophys. Res.*, *101*, 16,731-16,736, 1996.

Gormley, P. G., and M. Kennedy, Diffusion from a stream flowing through a cylindrical tube, *Proc. R. Ir. Acad.*, *52*, 163-169, 1949.

Hagen, D., P. Whitefield, J. Paladino, M. Trueblood, and H. Lilenfeld, Particulate sizing and emission indices for a jet engine exhaust sampled at cruise, *Geophys. Res. Lett.*, *25*, 1681-1684, 1998.

Hanisco, T. F., et al, The role of HO_x in super- and subsonic aircraft exhaust plumes, *Geophys. Res. Lett.*, *24*, 65-68, 1997.

Jensen, E. J., and O. B. Toon, The potential impact of soot particles from aircraft exhaust on cirrus clouds, *Geophys. Res. Lett.*, *24*, 249-251, 1997.

Jonsson, H. H., et al., Performance of a focused-cavity aerosol spectrometer for measurements in the stratosphere of particle size in the 0.06-2.0 μm diameter range, *J. Atmos. Oceanic Technol.*, *12*, 115-129, 1995.

Kärcher, B., Aviation-produced aerosols and contrails, *Surv. Geophys.*, *20*, 113-167, 1999.

Kärcher, B., and D. W. Fahey, The role of sulfur emission in volatile particle formation in jet aircraft exhaust plumes, *Geophys. Res. Lett.*, *24*, 389-392, 1997.

Kärcher, B., F. Yu, F. P. Schröder, and R. P. Turco, Ultrafine aerosol particles in aircraft plumes: Analysis of growth mechanisms, *Geophys. Res. Lett.*, *25*, 2793-2796, 1998a.

Kärcher, B., R. Busen, A. Petzold, F. P. Schröder, U. Schumann, and E. J. Jensen, Physicochemistry of aircraft-generated liquid aerosols, soot, and ice particles, 2, Comparison with observations and sensitivity studies, *J. Geophys. Res.*, *103*, 17,129-17,147, 1998b.

Kawa, S. R., Assessment of the effects of high-speed aircraft in the stratosphere: 1998, *NASA Tech. Publ., TP-1999-209237*, 149 pp., 1999. (Available from Nat. Tech. Inf. Serv., Springfield, Va.)

Lukachko, S. P., I. A. Waitz, R. C. Miake-Lye, R. C. Brown, and M. R. Anderson, Production of sulfate aerosol precursors in the turbine and exhaust nozzle of an aircraft engine, *J. Geophys. Res.*, *103*, 16,159-16,174, 1998.

Markowski, G. R., Improving the Twomey algorithm for inversion of aerosol measurement data, *Aerosol Sci. Technol.*, *7*, 127-141, 1988.

Miake-Lye, R. C., et al., SO_x oxidation and volatile aerosol in aircraft exhaust plumes depend on fuel sulfur content, *Geophys. Res. Lett.*, *25*, 1677-1680, 1998.

Paladino, J., P. Whitefield, D. Hagen, A. R. Hopkins, and M. Trueblood, Particle concentration characterization for jet engine emissions under cruise conditions, *Geophys. Res. Lett.*, *25*, 1697-1700, 1998.

Penner, J. E., D. H. Lister, D. J. Griggs, D. J. Dokken, and M. McFarland (Eds.), *Aviation and the Global Atmosphere: A Special Report of the IPCC Working Groups I and II*, Cambridge Univ. Press, New York, 1999.

Petzold, A., R., et al., Near-field measurements on contrail properties from fuels with different sulfur content, *J. Geophys. Res.*, *102*, 29,867-29,881, 1997.

Petzold, A., A. Döpelheuer, C. Brock, and F. Schröder, In situ observations and model calculations of black carbon emission by aircraft at cruise altitude, *J. Geophys. Res.*, *104*, 22,171-22,181, 1999.

Pueschel, R. F., S. Verma, G. V. Ferry, S. D. Howard, S. Vay, S. A. Kinne, J. Goodman, and A. W. Strawa, Sulfuric acid and soot particle formation in aircraft exhaust, *Geophys. Res. Lett.*, *25*, 1685-1688, 1998.

Pui, D. Y. H., K. L. Rubow, J.-K. Lee, and B. Y. H. Liu, Design of pressure reducing devices for high purity gas sampling, *Swiss Contam. Control*, *3*, 408-412, 1990.

Saros, M.T., R. J. Weber, J. J. Marti, and P. H. McMurry, Ultrafine aerosol measurement using a condensation nucleus counter with pulse height analysis, *Aerosol Sci. Technol.*, *25*, 200-213, 1996.

Schröder, F.P., and J. Ström, Aircraft measurements of sub micrometer aerosol particles (> 7 nm) in the midlatitude free troposphere and tropopause region, *Atmos. Res.*, *44*, 333-356, 1997.

Schröder, F. P., B. Kärcher, A. Petzold, R. Baumann, R. Busen, C. Hoell, and U. Schumann, Ultrafine aerosol particles in aircraft plumes: In situ observations, *Geophys. Res. Lett.*, *25*, 2789-2792, 1998.

Schröder, F. P., C. A. Brock, R. Baumann, A. Petzold, R. Busen, P. Schulte, and M. Fiebig, In situ studies on volatile jet exhaust particle emissions: Impact of fuel sulfur content and environmental conditions on nuclei mode aerosols, *J. Geophys. Res.*,*105*, 19,941-19,954, 2000.

Schumann, U., J. Ström, R. Busen, R. Baumann, K. Gierens, M. Krautstrunk, F. P. Schröder, and J. Stingl, In situ observations of particles in jet aircraft exhausts and contrails for different sulfur-containing fuels, *J. Geophys. Res.*, *101*, 6853-6869, 1996.

Stolzenburg, M.R., and P.H. McMurry, An ultrafine condensation nucleus counter, *Aerosol Sci. Technol.*, *14*, 48-65, 1991.

Tremmel, H. G., and U. Schumann, Model simulations of fuel sulfur conversion efficiencies in an aircraft engine: Dependence on reaction rate constants and initial species mixing ratios, *Aerosp. Sci. Technol., 3*, 417-430, 1999.

Weber, R. J., A. D. Clarke, M. Litchy, J. Li, G. Kok, R. D. Schillawski, and P. H. McMurry, Spurious aerosol measurements when sampling from aircraft in the vicinity of clouds, *J. Geophys. Res., 103*, 28,337-28,346, 1998.

Weisenstein, D. K., M. K. W. Ko, I. G. Dyominov, G. Pitari, L. Ricciardulli, G. Visconti, and S. Bekki, The effects of sulfur emissions from HSCT aircraft: A 2-D model intercomparison, *J. Geophys. Res., 103*, 1527-1547, 1998.

Wey, C. C., et al., Engine gaseous aerosol precursor and particulate at simulated flight altitude conditions, *NASA Tech. Memo., TM-1998-208509*, 1998.

Wilson J.C., E. D. Blackshear, and J. H. Hyun, The function and response of an improved stratospheric condensation nucleus counter, *J. Geophys. Res., 88*, 6781-6785, 1983.

Winklmayr, W., H.-C. Wang, and W. John, Adaption of the Twomey algorithm to the inversion of cascade impactor data, *Aerosol Sci. Technol., 13*, 322-331, 1990.

Yu, F., and R. P. Turco, The role of ions in the formation and evolution of particles in aircraft plumes, *Geophys. Res. Lett., 24*, 1927-1930, 1997.

Yu, F., and R. P. Turco, The formation and evolution of aerosols in stratospheric aircraft plumes: Numerical simulations and comparisons with observations, *J. Geophys. Res., 103*, 25,915-25,934, 1998a.

Yu, F., and R. P. Turco, Contrail formation and impacts on aerosol properties in aircraft plumes: Effects of fuel sulfur content, *Geophys. Res. Lett., 25*, 313-316, 1998b.

Yu, F., R. P. Turco, B. Kärcher, and F. P. Schröder, On the mechanisms controlling the formation and properties of volatile particles in aircraft wakes, *Geophys. Res. Lett., 25*, 3839-3842, 1998.

C. A. Brock, Department of Engineering, University of Denver, Denver, CO 80208. (cbrock@al.noaa.gov)

R. Busen, M. Fiebig, B. Kärcher, A. Petzold, and F. Schröder, Institut für Physik der Atmosphäre, Deutsche Luft- und Raumfahrt, Oberpfaffenhofen, D-92234 Weβling, Germany. (reinhold.busen @dlr.de; markus.fiebig@dlr.de; bernd.kaercher@dlr.de; andreas. petzold@dlr.de; franz.schroeder@dlr.de.)

(Received March 31, 2000; revised May 31, 2000;
accepted June 7, 2000.)